# Photoinduced electron transfer from enol silyl ethers to quinone. Part 1. Pronounced effects of solvent polarity and added salt on the formation of α-enones

**T. Michael Bockman, D. Shukla and Jay K. Kochi ***

*Department of Chemistry, University of Houston, Houston, TX 77204-5641, USA*

**The enol silyl ethers (ESE) of various ketones are efficiently oxidized to the corresponding α,β-unsaturated enones (E) when a dichloromethane solution containing equimolar amounts of chloranil is irradiated with filtered light ($\lambda_{exc}$ > 380 nm). The 1:1 adduct (A) of enol silyl ether and quinone is a byproduct, the structure of which is established by X-ray crystallography. Solvent polarity and added salts play a major role in establishing the product distribution between E and A. Such a medium effect, coupled with the ready isomerization of the kinetic–thermodynamic isomers derived from the silylation of 2-methylcyclohexanone, points to the cation radical of the enol silyl ether ($ESE^{\bullet+}$) as the reactive intermediate. A radical–ion pair mechanism involving the rapid one-electron oxidation of enol silyl ethers by photoactivated chloranil is discussed.**

## Introduction

The synthetic transformation of ketones to α,β-unsaturated carbonyl compounds (α-enones) can be carried out *via* their prior conversion to the corresponding enol silyl ethers;[1] and the subsequent oxidative removal of the β-hydrogen has been effected with such diverse reagents as trityl cation,[2] quinone (DDQ),[3] ceric ammonium nitrate,[4] iodosylbenzene–azide [5] and palladium(II) acetate.[6] Enol silyl ethers are also readily converted to α-enones with the aid of photoactivated quinones.[7] Indeed, the latter are directly related to a variety of other photosensitized transformations of enol silyl ethers (ESE), in which various photoactivated acceptors (A*) are involved in an initial electron transfer [eqn. (1)].[8–10]

$$ESE + A^* \xrightarrow{fast} ESE^{\bullet+} + A^{\bullet-} \qquad (1)$$

Since the cation radical ($ESE^{\bullet+}$) is also formed in the ready oxidation of enol silyl ethers with cerium(IV), silver(I), copper(II), *etc.*[11,12] (which are known one-electron oxidants), we need to inquire as to how such a reactive intermediate is converted to α-enones when the various quinones in eqn. (1) [*i.e.* A* = chloranil(tetrachloro-1,4-benzoquinone),dichlorobenzoquinone, benzoquinone, duroquinone, *etc.*] are quenched by enol silyl ethers. Among the various quinones, chloranil (CA) is especially useful since it is efficiently excited to its reactive triplet state [13] ($^3CA^*$), which has been identified as a powerful electron acceptor in a variety of photoinduced electron-transfer reactions.[14–17]

Particularly pertinent to this study is the effect of the structural variation of the enol (ketonic) moiety on the photoefficiency of enone formation. Furthermore, we exploit solvent and salt effects of the medium in specifically probing the dynamic behaviour of the radical–ion pairs formed according to eqn. (1). These investigations will thus set the phenomenological stage for delineating in detail the subsequent evolution of the transient radical–ion pair to the ultimate products by time-resolved spectroscopic techniques to be described in the following report.[18]

The various photochemical transformations sensitized by chloranil also have a more general bearing on the *thermal* reactions of organic substrates with high-potential quinones.[19] These include the dehydrogenation, oxidation, and oxidative addition [20,21] of electron-rich donors such as arenes,[22,23] alkenes,[24] amines,[25] alcohols [26] and organometallic compounds.[27]

## Results

Four classes of enol silyl ethers employed in this study were arbitrarily classified on the basis of (i) the ring size of the cycloalkanone, (ii) the substituents on silicon, (iii) the alkyl substitution pattern and (iv) an open-chain ketonic structure.

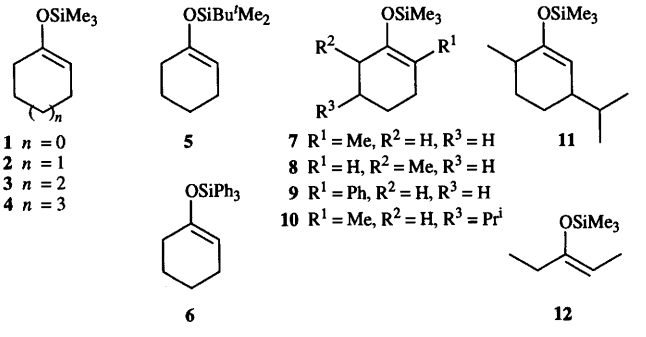


Thus the first series comprised the enol trimethylsilyl ethers of the homologous cyclopentanone (**1**), cyclohexanone (**2**), cycloheptanone (**3**) and cyclooctanone (**4**). In the second series, cyclohexanone enol trimethylsilyl ether **2** was compared to the *tert*-butyldimethylsilyl analogue **5** and the triphenylsilyl derivative **6**. Next, the location of the methyl, isopropyl, and phenyl substituents on the cyclohexanone enol trimethysilyl ether was considered in the behaviour of **7**–**11**. Finally, diethyl ketone enol trimethylsilyl ether **12** served as the representative acyclic alkanone.

### Spectral absorption of chloranil with and without enol silyl ether

The UV–VIS absorption spectrum of chloranil dissolved in dichloromethane consisted of a single (unresolved) band with its maximum centred at $\lambda_{max}$ = 375 nm and a molar extinction coefficient of $\varepsilon_{max}$ = 230 $dm^3\ mol^{-1}\ cm^{-1}$, as shown in Fig. 1. The same absorption band, with a slight spectral blue shift to $\lambda_{max}$ = 367 nm ($\varepsilon_{max}$ = 250 $dm^3\ mol^{-1}\ cm^{-1}$) was observed upon the dissolution of chloranil in acetonitrile, and it has been assigned to the local excitation of chloranil to its excited ($\pi\pi^*$) state.[28] The UV–VIS spectrum of chloranil was unchanged in

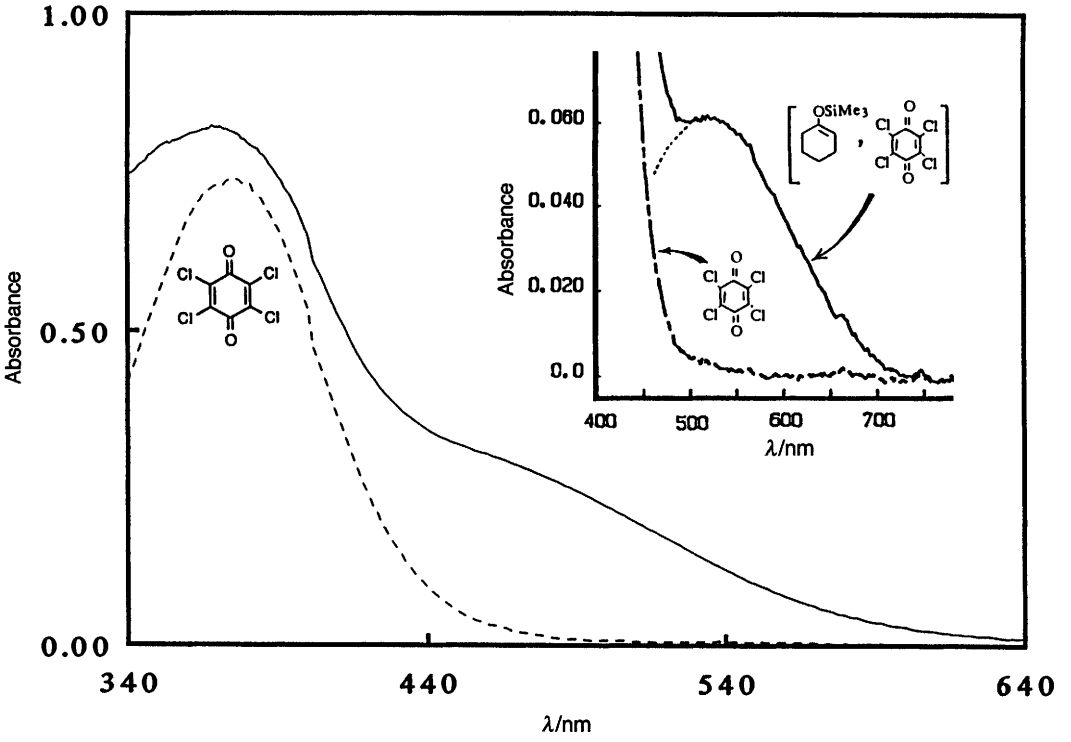


**Fig. 1** Absorption spectrum of 0.10 M chloranil in dichloromethane containing equimolar amount of enol silyl ether **2** (——) or no enol silyl ether (– – – –). Inset: Same solution with excess **2** added in order to elicit clearly the partially resolved charge-transfer spectrum of the EDA complex.

the presence of equimolar amounts of enol silyl ether, but a close inspection of Fig. 1 revealed the presence of an additional (very weak) band centred at $\lambda_{max}$ = 490 nm. Incremental additions of enol silyl ether was accompanied by a concomitant growth of the broad 490 nm band, in accord with its spectral assignment to the charge-transfer absorption of the 1:1 electron donor–acceptor or EDA complex that was rapidly formed according to eqn. (2).[10] The presence of two spectrally

$$CA + ESE \overset{K_{EDA}}{\rightleftharpoons} [ESE, CA] \qquad (2)$$

distinct absorption bands in Fig. 1—the local band of chloranil and the red-shifted charge-transfer band—allowed the selective photostimulation of the two transitions centred at 380 nm and 500 nm, respectively. Accordingly for the preparative photochemical experiments, the direct photoactivation of chloranil was effected with the focussed beam from a 500 W high pressure mercury lamp, which was first passed through a water filter to remove infrared light and then through a Pyrex sharp cutoff filter (Corning CS 3–75) to remove all ultraviolet light with $\lambda_{exc}$ < 380 nm. For the alternative excitation of the charge-transfer band, the concentration of enol silyl ether was increased and an extended cutoff filter (Corning CS 3–70) was used to remove all ultraviolet light with $\lambda_{exc}$ < 500 nm.

### Oxidation of cyclohexanone enol silyl ether by photoactivated chloranil

An equimolar solution of cyclohexanone enol trimethylsilyl ether **2** and chloranil was irradiated with visible light ($\lambda_{exc}$ > 380 nm) for 1–2 h. Periodic inspection of the UV–VIS spectrum of the photolysate indicated the monotonic disappearance of chloranil with $\lambda_{max}$ = 375 nm. The combined $^1$H NMR spectroscopic, GC–MS and HPLC analysis revealed the presence of cyclohex-2-enone[29] (**2E**) in 80% yield, as quantified by the internal standard technique. Transfer of the trimethylsilyl moiety upon the *oxidative elimination* of enol silyl ether **2** according to eqn. (3) was established by the isolation of mono-trimethylsilyl ether of tetrachlorohydroquinone.[30]

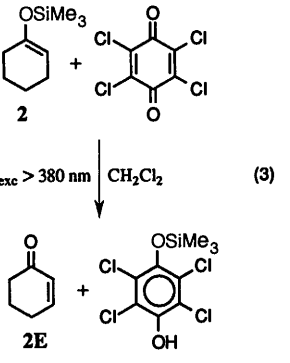


(3)

The presence of a byproduct (with molecular mass equal to the sum of chloranil and silyl ether **2**) was also detected in the GC–MS of the photolysate. Spectral ($^1$H NMR) comparison suggested the minor product to be the chloranil adduct **2A** analogous to that previously obtained from **2** and DDQ.[3a] It was separated by silica gel chromatography of the photolysate, and GC–MS analysis indicated the molecular weight of the isolated adduct to be 72 mass units less than that of the minor product **2A** of the photolysate—from which we inferred that hydrolytic loss of the trimethylsilyl group had occurred during chromatography. Accordingly, the molecular structure was established by the isolation of the crystalline adduct from chloranil and 2-methylcyclohexanone enol trimethylsilyl ether **7** (after chromatographic workup), followed by X-ray crystallographic analysis. The ORTEP diagram of the chloranil adduct in Fig. 2 shows the tetrachlorohydroquinone moiety to be O-bonded to the α-carbon of 2-methylcyclohexanone. We concluded from this structure that the byproduct **2A** resulted from the *oxidative addition* of cyclohexanone enol trimethylsilyl ether **2** to chloranil, according to eqn. (4).

The coproduction of enone **2E** and adduct **2A** was monitored by $^1$H NMR and GC analysis of small aliquots periodically extracted during the photoinduced reaction of cyclohexanone silyl ether **2** and chloranil. Indeed, Fig. 3 shows the temporal

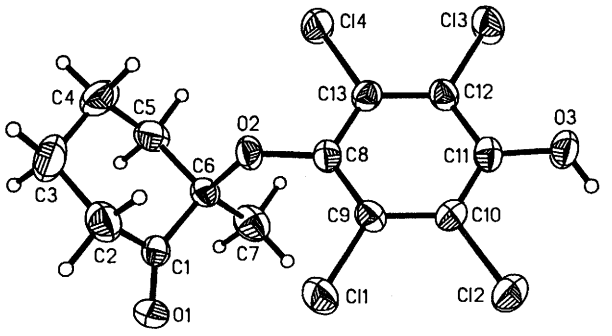


**Fig. 2** ORTEP diagram of the adduct derived from the oxidative addition of the enol silyl ether of 2-methylcyclohexanone to photoactivated chloranil (see text)

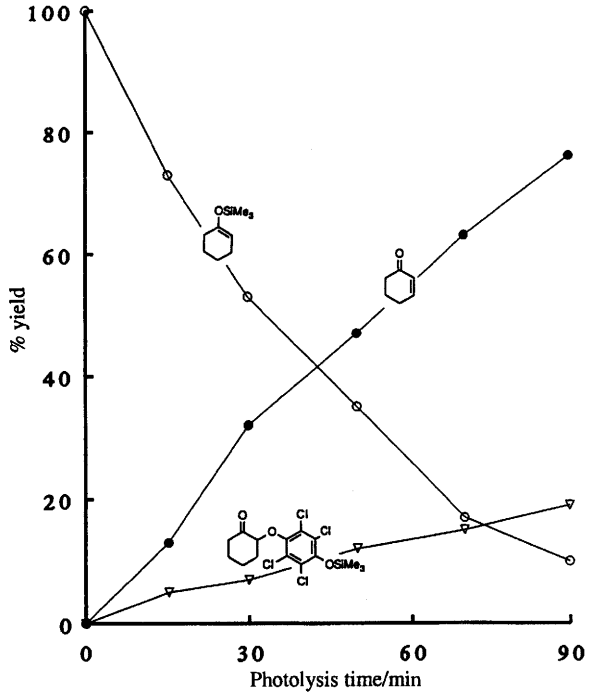


**Fig. 3** Time-dependent conversion of cyclohexanone enol trimethylsilyl ether (**2**) to cyclohexenone (**2E**) and adduct (**2A**) by photoactivated chloranil in dichloromethane at 25 °C

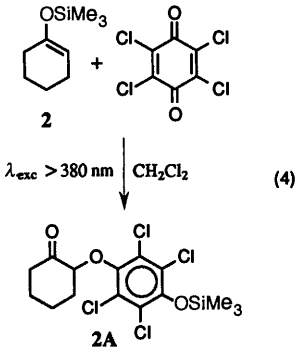


loss of the enol silyl ether to be accompanied by the concomitant formation of cyclohex-2-enone **2E** and adduct **2A**. The product ratio [**2E**]:[**2A**] remained constant throughout the photolysis to indicate that both α-enone and adduct were primary products on the timescale (1 h) of these experiments.

### Competition between oxidative elimination and addition of enol silyl ethers with chloranil

The four classes of enol silyl ethers were uniformly treated with chloranil under standard photochemical conditions (with $\lambda_{exc} > 380$ nm) in dichloromethane solutions. The photochemical yields of enone (**E**) and adduct (**A**) were determined by GC–MS and $^1$H NMR spectroscopic analysis (see Experimental section); and the distribution of these products in the photolysates is listed in Table 1. The excellent material balance (columns 4 plus 5), together with the results shown in Fig. 3, supported the parallel photochemical pathways leading to oxidative elimination and addition. The results in Table 1 show that the competition between oxidative elimination and addition of cycloalkanone enol ethers was highly dependent on the ring size—with the cyclopentanone and cyclohexanone enol ethers affording good yields of the corresponding enone (**E**), but the seven- and eight-membered analogues giving only poor yields. In each case, the deficit in the material balance was largely made up by the accompanying changes in the yields of adducts (**A**). Changes in alkyl and phenyl substitution on silicon exerted only a minor effect on the competition between oxidative elimination and addition (compare entries 1, 5 and 6 in Table 1).

**Table 1** Photoinduced oxidation of enol silyl ethers with chloranil in dichloromethane[a]

| Enol silyl ether | Irradiation time/h | Conversion (%)[b] | Products (%) | |
|---|---|---|---|---|
| | | | Enone (**E**) | Adduct (**A**)[c] |
| **1** | 1.0 | 100 | 83 | 11 |
| **2** | 1.0 | 100 | 80 | 20 |
| **3** | 1.0 | 100 | 19 | 73 |
| **4** | 1.0 | 100 | 10 | 80 |
| **5** | 1.0 | 100 | 75 | *d* |
| **6** | 2.0 | 100 | 60 | 28 |
| **7** | 22 | 89 | 65 | 23[e] |
| **8** | 1.0 | 87[f] | 72 | 10 |
| **9** | 25 | 75 | 65 | *d* |
| **10** | 15 | 60 | 51 | *d* |
| **11** | 1.0 | 80 | 75 | 5 |
| **12** | 0.5 | 100 | 5 | 90 |

[a] Upon irradiation with $\lambda > 380$ nm of chloranil and enol silyl ether (both 0.01 M). [b] Based on unreacted enol silyl ether and enone (**E**) determined by GC analysis. [c] Yield of adduct (**A**) determined by $^1$H NMR spectroscopic analysis. [d] Not quantified. [e] See the structure in Fig. 2. [f] Unreacted enol silyl ether was isomerized to **7**.

Although methyl and phenyl substituents, particularly on the α-carbon (see entries 7, 9 and 10), did not materially affect the relative branching of enones to adducts, the efficiency of the overall photochemical process was significantly diminished, as indicated by the longer irradiation times required to achieve the high conversions in Table 1, column 3. Particularly noteworthy was the striking contrast provided by the isomeric methylcyclohexanone enol ethers, in which the (thermodynamic) isomer **7** substituted in the 2-position required a long period of irradiation (22 h) to achieve (~90%) conversion under conditions in which the 6-methyl substituted (kinetic) isomer **8** required less than an hour. Spectral examination of the photolysate from the kinetic isomer **8** revealed that rearrangement led to residual amounts of the more stable isomer **7**, *i.e.* as shown in eqn. (5). Indeed, the periodic

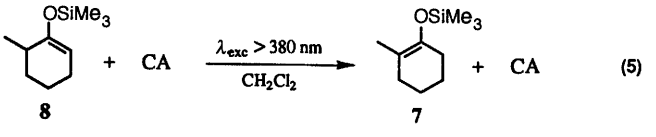


monitoring of the photolysate from **8** indicated the facile isomerization in eqn. (5) was concurrent with oxidative elimination and addition, as shown by the product ratio in Fig. 4 that was more or less independent of the irradiation period.

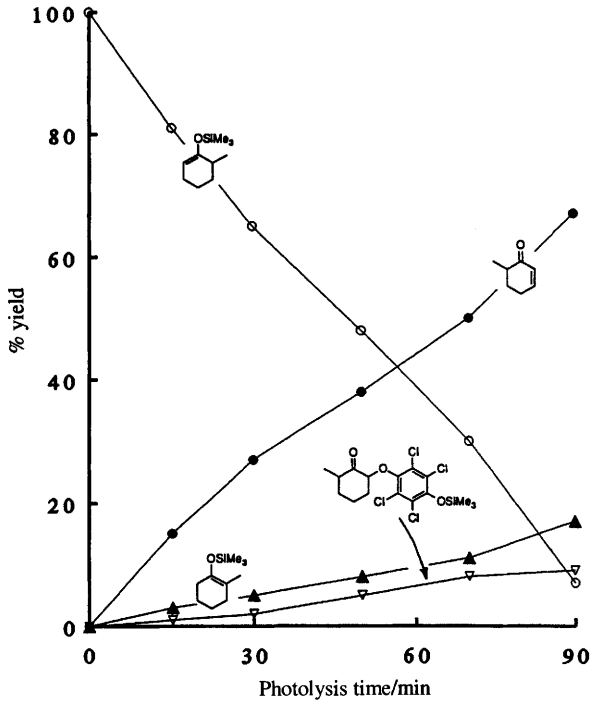


**Fig. 4** Oxidative elimination and addition of 6-methylcyclohexenyl trimethylsilyl ether (**8**) with photoactivated chloranil, showing the concomitant isomerization to 2-methylcyclohexenyl silyl ether (**7**)

**Table 2** Oxidative elimination and addition of enol silyl ethers with chloranil in acetonitrile[a]

| Enol silyl ether | Irradiation time/h | Conversion (%)[b] | Products (%) | |
|---|---|---|---|---|
| | | | Enone (**E**) | Adduct (**A**) |
| **2** | 1 | 100 | 19 | 79 |
| **3** | 1 | 100 | 11 | 87 |
| **5** | 1 | 95 | 80 | 15 |
| **6** | 1 | 30 | 20 | 7 |
| **7** | 25 | 100 | 11 | 70 |
| **9** | 25 | 73 | 35 | — |
| **11** | 15 | 71 | 38 | — |

[a] Under the conditions described in Table 1. [b] Analysis of enol silyl ethers and enones (GC) and adducts ($^1$H NMR spectroscopy) as in Table 1.

### Effects of solvent polarity and added salt on oxidative elimination *versus* oxidative addition

Although the change in the medium from dichloromethane to acetonitrile represented a sizeable enhancement in solvent polarity,[31] the results in Table 2 show no significant difference in the photochemical *efficiencies* with which the various enol silyl ethers were oxidatively converted by chloranil to the corresponding enones (**E**) and adducts (**A**). Thus in each case, the time/conversion observed in dichloromethane (Table 1, columns 2 and 3) paralleled those obtained in acetonitrile (Table 2). However, the product *distributions* between α-enone and adduct in acetonitrile were significantly altered relative to those obtained in dichloromethane. For example, the prototypical enol silyl ether derived from cyclohexanone (**2**), which gave a high yield (80%) of enone **2E** (and only 20% adduct **2A**) in dichloromethane, produced only a minor amount (19%) of α-enone (but 79% adduct) in acetonitrile. Oxidative elimination was also reduced for the trimethylsilyl ethers of cycloheptanone and 2-methylcyclohexanone in acetonitrile, and the enone : adduct ratios were essentially inverted relative to those obtained in dichloromethane (compare columns 4 and 5 in Tables 1 and 2). On the other hand, the enol ethers substituted with bulky triphenylsilyl and *tert*-butyldimethylsilyl groups (**5** and **6**) yielded essentially the same product distributions as those observed in parallel reactions carried out in dichloromethane solution.

**Table 3** Quantum yields for the loss of enol silyl ether and the formation of α-enone[a]

| Enol silyl ether | Solvent | Quantum yields | | |
|---|---|---|---|---|
| | | $\Phi_{loss}$[b] | $\Phi_{enone}$[c] | $\Phi_{adduct}$[d] |
| **1** | $CH_2Cl_2$ | 0.85 | 0.68 | 0.17 |
| **2** | $CH_2Cl_2$ | 0.83 | 0.68 | 0.15 |
| | $CH_3CN$ | 0.79 | 0.04 | 0.75 |
| **3** | $CH_2Cl_2$ | 0.68 | 0.03 | 0.65 |
| **4** | $CH_2Cl_2$ | 0.65 | 0.01 | 0.64 |
| **5** | $CH_2Cl_2$ | 0.87 | 0.63 | 0.24 |
| | $CH_3CN$ | 0.90 | 0.72 | 0.18 |
| **6** | $CH_2Cl_2$ | 0.35 | 0.28 | 0.07 |
| | $CH_3CN$ | 0.50 | 0.48 | 0.02 |
| **7** | $CH_2Cl_2$ | 0.08 | 0.07 | 0.01 |
| | $CH_3CN$ | 0.09 | 0.01 | 0.08 |
| **8** | $CH_2Cl_2$ | 0.85 | 0.63 | 0.22 |
| | $CH_3CN$ | 0.68 | 0.03 | 0.65 |
| **9** | $CH_2Cl_2$ | 0.05 | 0.04 | 0.01 |

[a] From the irradiation ($\lambda$ = 360 ± 10 nm) of equimolar solutions of chloranil and enol silyl ether (0.02 M). Photon fluxes were determined with potassium ferrioxalate as actinometer. [b] Quantum yields for the conversion of silyl enol ether (±0.07). [c] Quantum yield for α-enone formation (±0.05). [d] Quantum yield for adduct formation calculated on the basis of ($\Phi_{loss} - \Phi_{enone}$), see text.

The alteration of the product distribution from predominant α-enone to predominant adduct could also be effected in dichloromethane solution by the addition of electrolytes (salts) to the reaction mixture. For example, the photoinduced oxidation of cyclohexanone enol silyl ether **2** by chloranil when carried out in dichloromethane containing 0.1 M tetrabutylammonium hexafluorophosphate ($TBA^+PF_6^-$) yielded adduct **2A** in 80% yield [eqn. (6)], which was the same as that obtained in

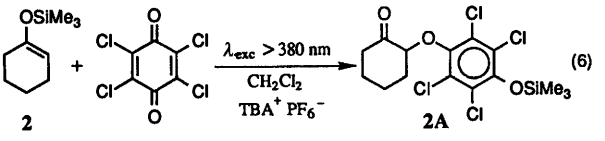


acetonitrile (Table 2); and only minor amounts (20%) of cyclohexenone **2E** were observed.

### Quantum efficiency of the oxidative elimination of enol silyl ethers by chloranil

Quantitative measures of the photoefficiency for oxidative elimination were evaluated from the quantum yields for the consumption of enol silyl ether ($\Phi_{loss}$) and the formation of enone ($\Phi_{enone}$) measured with the aid of monochromatic light beam, with $\lambda_{exc}$ = 360 ± 5 nm, that was obtained by passing the output from a 500 W xenon lamp through a narrow-band interference filter. The photon flux was determined by ferrioxalate actinometry according to the method of Hatchard and Parker.[32] The enol silyl ether and α-enone were analysed by quantitative GC using dodecane as the internal standard. Conversions were kept to less than 20% to minimize any secondary photolysis of the products.

The measured quantum yields for the overall conversion of enol silyl ether in Table 3 were highly dependent on the substitution pattern around the double bond. Thus, efficient photoconversions with $\Phi_{loss} \approx 0.8$ were characteristic of enol silyl ethers **1**–**5** and **8** that were unsubstituted in the 2-position. On the other hand, 2-methyl- and 2-phenyl-cyclohexenyl trimethylsilyl ethers **7** and **9** gave the significantly reduced efficiencies of $\Phi_{loss}$ = 0.09 and 0.05, respectively. Such a diminution in $\Phi_{loss}$ quantitatively reflected the long photolysis

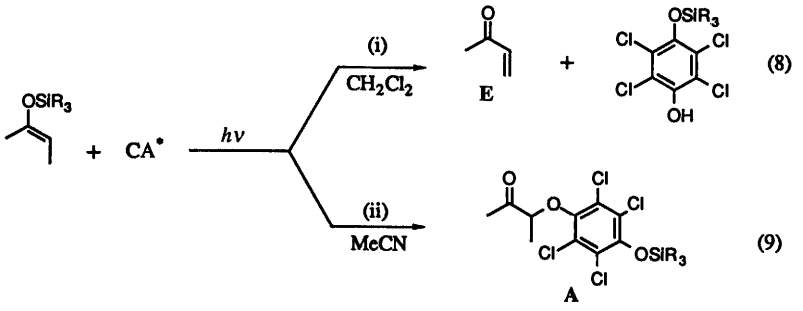


Scheme 1

times required to effect the photoconversion of these substrates in Tables 1 and 2. There was only a modest effect of the silyl moiety on $\Phi_{loss}$—the triphenylsilyl ether **6** being only slightly less reactive than the corresponding trimethylsilyl **2** or *tert*-butyldimethylsilyl **5** ethers.

**Solvent effect.** There was no appreciable effect of solvent polarity on the photochemical conversion, and the quantum yield for the consumption of enol silyl ether was essentially the same in dichloromethane and acetonitrile, as indicated by the values of $\Phi_{loss}$ in Table 3, column 3. The quantum yield for oxidative elimination ($\Phi_{enone}$ in column 4) was, however, much diminished in the more polar solvent. These reduced values of $\Phi_{enone}$ thus mirrored the results of the preparative experiments in which the diminished importance of α-enone relative to adduct generally prevailed in the more polar acetonitrile (Table 2) relative to that observed in dichloromethane (Table 1). Values of $\Phi_{enone}$ for the bulky triphenylsilyl and *tert*-butyldimethylsilyl ethers of cyclohexanone (**5** and **6**) were more or less unaffected by solvent polarity, and in each case the rather invariant value of $\Phi_{loss}$ reflected the efficient formation of α-enone in both dichloromethane and acetonitrile.

**Salt effect.** The effect of the innocuous salt, tetrabutylammonium hexafluorophosphate, on the quantum yields for the loss of cyclohexanone enol silyl ether **2** and the formation of cyclohex-2-enone in dichloromethane is presented in Table 4. The results in column 2 show that the quantum yield for the conversion of the enol silyl ether was singularly unaffected by the presence of increasing concentrations of $TBA^+PF_6^-$. On the other hand, the progressive addition of salt resulted in the monotonic diminution in the quantum yield for enone formation—the value of $\Phi_{enone}$ dramatically decreasing by five-fold when 0.1 M $TBA^+PF_6^-$ was present. The latter was thus in accord with the product changeover from enone to adduct in the presence of salt, as described in eqns. (3) and (6), respectively.

### Charge-transfer activation of the chloranil complex with enol silyl ether

Solutions of chloranil containing equimolar amounts of enol silyl ethers **2** or **8** in either dichloromethane or acetonitrile remained unchanged for prolonged periods at 23 °C. In an attempt to induce a photoreaction, these solutions were selectively irradiated with filtered light ($\lambda_{exc}$ > 500 nm) to excite only the charge-transfer absorption ($h\nu_{CT}$) in Fig. 1, and not the local transition of either chloranil or the enol silyl ether. Under these conditions, no change in the UV–VIS spectrum of the photolysate was observed even after long (48 h) irradiation times. Chloranil and the enol silyl ether could be recovered quantitatively upon the workup of the reaction mixture. (See the Experimental section for details of the analysis.) Accordingly, we concluded that photostimulation of the EDA complex [eqn. (2)] *via* the charge-transfer transition merely led to a photostationary state,[33] as in eqn. (7), from which essentially no productive photochemistry derived.

**Table 4** Salt effect on the quantum efficiency for oxidative elimination and addition[a]

| | Quantum yield | | |
|---|---|---|---|
| $[TBA^+ PF_6^-]$/M[b] | $\Phi_{loss}$[c] | $\Phi_{enone}$[d] | $\Phi_{adduct}$[e] |
| 0 | 0.83 | 0.68 | 0.15 |
| 0.014 | 0.80 | 0.50 | 0.30 |
| 0.03 | 0.78 | 0.27 | 0.51 |
| 0.055 | 0.85 | 0.18 | 0.67 |
| 0.10 | 0.78 | 0.13 | 0.65 |

[a] Upon the irradiation of a dichloromethane solution of 0.02 M chloranil and 0.02 M cyclohexenyl trimethylsilyl ether (**2**) with monochromatic light (360 ± 10 nm). [b] Concentration of the added inert salt, tetrabutylammonium hexafluorophosphate. [c] Quantum yields for conversion of **2** (±0.05), and [d] the formation of cyclohex-2-enone (±0.07). [e] See Table 3.

$$[ESE, CA] \overset{h\nu_{CT}}{\rightleftharpoons} [ESE^{\bullet+}, CA^{\bullet-}] \qquad (7)$$

## Discussion

The preparative photochemical studies of the various enol silyl ethers by actinic irradiation with $\lambda_{exc}$ > 380 nm result directly from the prior photoactivation of chloranil.[34] Photoexcited chloranil (CA*) then reacts with enol silyl ethers *via* two competing pathways, namely (i) *oxidative elimination* to yield the enone **E** and (ii) *oxidative addition* to yield the adduct **A**, as presented generically in Scheme 1.

The results in Tables 1 and 2 indicate that the partitioning between the two pathways is controlled by solvent polarity—with non-polar solvents, such as dichloromethane, favouring oxidative elimination and polar solvents, such as acetonitrile, favouring oxidative addition. More strikingly, the mere presence of an inert electrolyte such as tetrabutylammonium hexafluorophosphate ($TBA^+PF_6^-$) in dichloromethane is sufficient to divert the predominant pathway leading to oxidative elimination in dichloromethane to adduct formation (Table 4). In addition to the pronounced medium effects of solvent polarity and added salt, the competition between oxidative elimination and addition is highly dependent on the structure of the enol silyl ether (Table 3). Accordingly, let us consider how solvent polarity, as well as added salts, and the structural effects of the specific enol silyl ethers modulate (i) the overall efficiency of the photoreaction, as measured by $\Phi_{loss}$ in Table 3, and (ii) the product partitioning between enone and adduct in Scheme 1.

### Environmental and structural effects on the modulation of oxidative elimination *versus* oxidative addition

**Solvent polarity.** For the prototypical trimethylsilyl ether **2** derived from cyclohexanone, the photoefficiency is unaffected by solvent polarity—the value of $\Phi_{loss}$ being the same in a non-polar solvent such as dichloromethane as in the polar

acetonitrile. Indeed, this pattern for $\Phi_{loss}$ prevails generally for all the enol silyl ethers in Table 3. In contrasting, the distribution between enone (**E**) and adduct (**A**) is highly dependent on solvent polarity—the product ratios [**E**]:[**A**] decidedly decreasing on changing the solvent from dichloromethane (Table 1) to acetonitrile (Table 2). The marked solvent effect on the product distribution is quantitatively evaluated by the decreasing values of $\Phi_{enone}$ in Table 3. Most importantly, the opposed (distinctive) response of the activation process ($\Phi_{loss}$) and product distribution ($\Phi_{enone}$) to solvent polarity indicates that the photolysis initially results in a *common intermediate*, which is subsequently partitioned to enone and adduct.

**Added salt.** The presence of inert salt ($TBA^+PF_6^-$) during the photolysis in dichloromethane mimics the medium change to a more polar solvent; and the overall photoefficiency as measured by $\Phi_{loss}$ in Table 4 is unaffected by varying amounts of added $TBA^+PF_6^-$. In contrasting, the product distribution in dichloromethane is highly sensitive to the presence of added salt. Thus the value of $\Phi_{enone}$ diminishes monotonically with added $TBA^+PF_6^-$, and at relatively high (0.1 M) concentrations $\Phi_{enone}$ reaches a value (0.1) close to that (0.04) obtained in acetonitrile (with no added salt). The parallel response elicited by solvent polarity and added salt on the dichotomy between $\Phi_{loss}$ and $\Phi_{enone}$ is symptomatic of the modulation of ionic behaviour and it thus points to the ion pair as the *common intermediate* in the oxidation of enol silyl ethers by photoactivated chloranil.

**Enol silyl ether structure.** The observed lack of regioselectivity for enol silyl ether **8** coincides with its rapid isomerization to **7** during the course of photooxidation (see Fig. 4). Otherwise, the purely thermal isomerization of the kinetic isomer **8** to the thermodynamic isomer **7** occurs too slowly to account for the results in Table 1 (entries 7 and 8). On the other hand, the cation radical of the kinetic enol silyl ether $\mathbf{8}^{\bullet+}$ is known to be readily converted to the cation radical of the thermodynamic isomer $\mathbf{7}^{\bullet+}$ by a fast 1,3-prototropic shift [eqn. (10)].[35,36] Such an

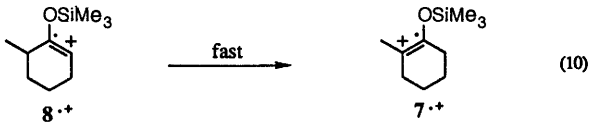

(10)

efficient isomerization of the cation radical $\mathbf{8}^{\bullet+}$ to $\mathbf{7}^{\bullet+}$ is thus consistent with a pathway involving the facile one-electron oxidation of the enol silyl ether.[10]

**Formation of the radical–ion pair as the common intermediate**

The combined effects of solvent polarity, added salt and enol silyl ether structures point to the cation radical of the enol silyl ether as the common intermediate in their oxidation by photoactivated chloranil CA*. As such, a photoinduced electron transfer as depicted in eqn. (11) would be consistent

$$ESE + CA^* \xrightarrow{k_{ET}} ESE^{\bullet+} + CA^{\bullet-} \qquad (11)$$

with a variety of other photosensitized transformations of enol silyl ethers.[8–10] If so, the various facets of oxidative elimination–addition that result from changes in the various structures of enol silyl ethers in Tables 1 and 2 must be related to the distinctive behaviour of the cation radicals ($ESE^{\bullet+}$). For example, the fact that enol silyl ethers **1** and **2** derived from five- and six-membered cyclic ketones in Table 1 yield principally enones (*i.e.* $\Phi_{loss} \approx \Phi_{enone}$) must be reconciled with the observation that seven- and eight-membered analogues afford adducts almost exclusively ($\Phi_{loss} \approx \Phi_{adduct}$). Moreover, all of the enol silyl ethers derived from cyclohexanone (**2**, **5**, **6**) yield α-enones in dichloromethane, whereas in acetonitrile the trimethysilyl ether **2** yields the adduct under conditions in which the *tert*-butyldimethylsilyl and triphenylsilyl analogues **5** and **6**, respectively, afford principally α-enones. Likewise, low quantum yields for $\Phi_{loss}$ characterize the reactivity of enol silyl ethers **7** and **9** with 2-methyl or 2-phenyl substituents, but their partitioning to α-enones and adducts is the same as that observed with the prototypical enol silyl ether **2** (and they are subject to the same modulation by solvent polarity). Each of these distinctive facets of enol silyl ether reactivity necessarily relates to the behaviour of the corresponding cation radical ($ESE^{\bullet+}$) subsequent to its formation. In particular, the ion-pair dynamics associated with the photoinduced electron transfer in eqn. (11) must be examined. Accordingly, the following paper[18] will describe how the direct observation of the intermediates by time-resolved spectroscopy will allow these dynamic processes to be identified in detail.

**Table 5** Thermodynamics for the quenching of chloranil triplet and the back electron transfer in radical-ion pairs

| Silyl enol ether | $\Phi_{loss}$ [a] | $E^\circ_{ox}$ [b]/V | $E_i$ [c]/eV | $-\Delta G^\circ_{ET}$ [d]/kcal mol$^{-1}$ | $-\Delta G^\circ_{BET}$ [e]/kcal mol$^{-1}$ |
|---|---|---|---|---|---|
| **1** | 0.85 | 1.39 | 8.3 | 17 | 31 |
| **2** | 0.83 | 1.47 | 8.4 | 15 | 33 |
| **3** | 0.68 | 1.56 | 8.3 | 13 | 36 |
| **7** | 0.08 | 1.20 | 7.9 | 21 | 27 |
| **9** | 0.05 | 1.16 [f] | 7.5 [f] | 22 | 26 |

[a] Quantum yield for the conversion of silyl enol ether in dichloromethane from Table 3. [b] Thermodynamic oxidation potentials (*vs.* SCE) in dichloromethane (see Experminental section), and [c] gas-phase ionization potentials from Ref. 10. [d] Driving force for the electron-transfer quenching of chloranil triplet, calculated as $-\Delta G^\circ_{ET} = F[E^\circ_{red}(CA) + E^\circ_{ox}(\text{silyl ether})] + E_T$, where $E^\circ_{red}(CA)$ is the reduction potential of chloranil (+0.02) and $E_T$ is the triplet energy (2.13 eV) of chloranil. [e] Driving force for back electron transfer in the radical–ion pair, taken as $-\Delta G^\circ_{BET} = F[E^\circ_{ox}(\text{silyl ether}) + E^\circ_{red}(CA)]$. [f] Taken to be the same as $E_i$ for the trimethylsilyl ether derived from β-tetralone in Ref. 10.

**Driving force for electron transfer from enol silyl ethers to photoactivated chloranil**

The viability of the electron-transfer mechanism for the oxidation of enol silyl ethers by photoactivated chloranil according to eqn. (11) is evaluated from the donor strength of ESE and the acceptor strength of CA*. Thus, the thermodynamic driving force for electron transfer can be calculated as[37] $-\Delta G_{ET} = F\,[E^\circ_{red}(CA) + E^\circ_{ox}(ESE)] + E_T$, where $E^\circ_{ox}$ (ESE) is the oxidation potential of the enol silyl ether,[38] $E^\circ_{red}(CA)$ is the reduction potential of chloranil and $E_T$ is the triplet energy of chloranil.[39] For all the enol silyl ethers in Table 5, the electron transfer in eqn. (11) is consistently exergonic, as given by the values of $-\Delta G_{ET}$ in the range of 13 to 22 kcal mol$^{-1}$.†

Although the quantum yields in Table 3 for the oxidative conversion of enol silyl ethers are high (*e.g.* $\Phi_{loss} = 0.80$ for **2**), they are significantly less than unity. Since the formation of the radical ion pair in eqn. (11) occurs with unit efficiency,[18] back electron transfer (BET) must be the (minor) process that returns the radical–ion pair to the starting material [eqn. (12)]. Indeed,

$$ESE^{\bullet+} + CA^{\bullet-} \xrightarrow{k_{BET}} ESE + CA \qquad (12)$$

back electron transfer is commonly observed in photoinduced electron transfer, and it has been the subject of a variety of time-resolved spectroscopic studies.[40,41] As evaluated here, the efficiency of back electron transfer is simply given as $\Phi_{BET} =$

† 1 cal = 4.184 J.

$(1 - \Phi_{loss})$ in Table 5, and typically the value of $\Phi_{BET}$ is 0.20 in dichloromethane and 0.10 in acetonitrile for enol silyl silyl ether **2**. The driving force for back electron transfer can be calculated as $-\Delta G_{BET} = F[E^{\circ}_{ox}(ESE) - E^{\circ}_{ox}(CA^{\bullet -})]$, where $E^{\circ}_{ox}(CA^{\bullet -})$ is the oxidation potential of the chloranil anion radical.[42] First, it should be noted that the values of $-\Delta G_{BET}$ are all positive to indicate highly exergonic driving forces for back electron transfer. Thus, the ion-pair pathways leading to oxidative elimination–addition in Scheme 1 must occur in competition with this highly favourable deactivation to regenerate the starting materials. Secondly, the back electron transfer with $\mathbf{7}^{\bullet +}$ and $\mathbf{9}^{\bullet +}$ derived from the 2-substituted enol silyl ethers are substantially less exothermic than that from the unsubstituted analogue $\mathbf{2}^{\bullet +}$. According to recent studies,[43,44] such a reduced driving force is associated with increased rates of back electron transfer.[45] In order to explain the high photoefficiency ($\Phi_{loss}$), despite the (expectedly) rapid rate of back electron transfer, we note that electron transfer occurs from photoactivated chloranil *via* its triplet state.[46] Since the radical–ion pair in eqn. (11) is formed with parallel spins, back electron transfer in eqn. (12) actually represents a composite step which includes a slower intersystem crossing[47] to a singlet state prior to back electron transfer. As a result, alternative ion-pair processes leading to oxidative elimination–addition could easily compete with the 'energetically favourable' back electron transfer. Such an entropic factor also accounts for the highly inefficient oxidative elimination–addition of enol silyl ethers and chloranil *via* the direct photoactivation of the EDA complex in eqn. (7). Since the charge-transfer transition occurs with no change in spin multiplicity, the radical–ion pair is formed in the singlet state, from which the values of $-\Delta G_{BET}$ in Table 5 predict the back electron transfer to be rapid.

## Experimental

### Materials

Tetrachlorobenzoquinone (chloranil, Aldrich) was purified by recrystallization from benzene, followed by vacuum sublimation. Chlorotrimethylsilane (TMSCl, Aldrich), sodium iodide (Aldrich), and the cyclic ketones, cyclohexanone, cyclopentanone, cyclooctanone, 2-methylcyclohexanone, and 2-phenylcyclohexanone (Aldrich) were used as received. The silyl enol ethers in this study were prepared by silylation of the cyclic ketones with TMSCl in the presence of triethylamine and sodium iodide, according to the general procedure of Cazeau *et al.*[48] Typically, the ketone (100 mmol) was added to a stirred solution of sodium iodide (18.6 g, 124 mmol) in dry acetonitrile (150 ml) that was maintained under an argon atmosphere. When the sodium iodide was completely dissolved, triethylamine (17 ml, 125 mmol) was added, followed by chlorotrimethylsilane (16 ml, 125 mmol). An exothermic reaction ensued, and the temperature rose to *ca.* 40–50 °C. The reaction mixture was stirred for 0.5 h and extracted with light petroleum (100 ml). Ice–water (50 ml) was added to the acetonitrile phase, which was then extracted with light petroleum (2 × 50 ml). The combined light petroleum extracts were washed with ice–water and dried over magnesium sulfate. The solvent was removed *in vacuo* to yield the crude silyl ether as a yellow oil. The silyl enol ethers were purified by fractional distillation under reduced pressure to afford colourless liquids, which were characterized by GC–MS and by comparison of their $^1$H NMR‡ spectra with those previously reported. *Cyclohex-1-enyl trimethylsilyl ether* **2**. $\delta_H(CDCl_3)$ 4.79 (t, 1 H,) 1.3–2.0 (m, 8 H), 0.11 (s, 9 H); GC–MS: 170, $M^{\bullet +}$, calculated for $C_9H_{18}OSi$, 170. *Cyclohept-1-enyl trimethylsilyl ether* **3**. $\delta_H(CDCl_3)$ 4.95 (t, 1 H, *J* 6.3), 1.3–2.2 (m, 10 H), 0.08 (s, 9 H); GC–MS: 184, $M^{\bullet +}$, calculated for $C_{10}H_{20}OSi$: 184. *Cyclooct-1-enyl trimethylsilyl ether* **4**. $\delta_H(CDCl_3)$ 4.68 (t, 1 H, *J* 8.0), 1.1–2.3 (m, 12 H), 0.13 (s, 9 H); GC–MS: 198, $M^{\bullet +}$, calculated for $C_{11}H_{22}OSi$: 198. *Cyclopent-1-enyl trimethylsilyl ether* **1**. $\delta_H(CDCl_3)$ 4.56 (br t, 1 H), 1.5–2.3 (m, 6 H), 0.14 (s, 9 H); GC–MS: 156, $M^{\bullet +}$; calculated for $C_8H_{16}OSi$: 156. *1-Ethylprop-1-enyl trimethylsilyl ether* **12**. $\delta_H(CDCl_3)$ 4.45 (q, 1 H, *J* 6.6), 1.94 (q, 2 H, *J* 8.0), 1.44 (d, 3 H, *J* 6.6), 0.93 (t, 3 H, *J* 8.0), 0.11 (s, 9 H); GC–MS: 158, $M^{\bullet +}$; calculated for $C_8H_{18}OSi$: 158.

*2-Methylcyclohex-1-enyl trimethylsilyl ether* **7**. $\delta_H(CDCl_3)$ 1.80–2.15 (m, 4 H), 1.45–1.70 (m, 7 H), 0.15 (s, 9 H); GC–MS: 184, $M^{\bullet +}$; calculated for $C_{10}H_{20}OSi$: 184. The cyclohexenyl ethers with triphenylsilyl and *tert*-butyldimethylsilyl substituents were prepared by the procedure described above, but using 125 mmol of chlorotriphenylsilane (Aldrich) and chloro-*tert*-butyldimethylsilane, respectively, in place of chlorotrimethylsilane. *Cyclohex-1-enyl* tert-*butyldimethylsilyl ether* **5**. $\delta_H(CDCl_3)$ 4.79 (t, 1 H, *J* 3.4), 1.6–2.3 (m, 8 H), 0.87 (s, 9 H), 0.09 (s, 6 H); GC–MS: 212, $M^{\bullet +}$; calculated for $C_{12}H_{24}OSi$: 212. *Cyclohex-1-enyl triphenylsilyl ether* **6**. $\delta_H(CDCl_3)$ 7.32–8.04 (m, 15 H), 5.11 (t, 1 H, *J* 4.0), 1.39–2.39 (m, 8 H); GC–MS: 356, $M^{\bullet +}$; calculated for $C_{24}H_{24}OSi$: 356. 6-Methylcyclohex-1-enyl trimethylsilyl ether was prepared by treatment of the lithium enolate of 2-methylcyclohexanone with chlorotrimethylsilane, according to the procedure of Fleming and Paterson.[49] *6-Methylcyclohex-1-enyl trimethylsilyl ether* **8**. $\delta_H(CDCl_3)$ 4.79 (t, 1 H, *J* 3.5), 1.90–2.35 (m, 3 H), 1.24–1.9 (m, 4 H), 1.07 (d, 3 H, *J* 7), 0.21 (s, 9 H); GC–MS: 184, $M^{\bullet +}$; calculated for $C_{10}H_{20}OSi$: 184.

Cyclohex-2-enone, cyclopent-2-enone, cyclohept-2-enone, and cyclooct-2-enone from Aldrich Chemical Co. were used as received. The substituted ketones identified as 2-methyl-, 6-methyl- and 2-phenyl-cyclohex-2-enones were obtained by oxidation of 2-methyl-, 6-methyl- and 2-phenyl-cyclohexenyl trimethylsilyl ethers, respectively, with dichlorodicyanobenzoquinone (DDQ). Typically, a solution of dry 2,4,6-collidine (2,4,6-trimethylpyridine) (2.06 g, 17 mmol) in dry benzene (10 ml) was added dropwise over a period of 5 min to a stirred solution of DDQ (3.53 g, 16 mmol) in benzene (50 ml) under an atmosphere of argon. After 0.5 h, a solution of the silyl enol ether (10 mmol) in benzene (10 ml) was added over 20 min to the reaction mixture. The dark red solution was stirred for 6 h and partitioned between 1 M sodium hydroxide solution (25 ml) and diethyl ether (100 ml). The aqueous layer was extracted twice with 100 ml portions of diethyl ether, and the organic fractions were combined and washed successively with 1 M sodium hydroxide solution (2 × 25 ml) and 1 M hydrochloric acid (100 ml). The organic extracts were dried with anhydrous magnesium sulfate. The solvent was removed *in vacuo* to afford the crude enone, which was purified by vacuum distillation. *6-Methylcyclohex-2-enone*. $\delta_H(CDCl_3)$ 6.96 (dt, 1 H, *J* 10 and 4), 5.98 (dt, 1 H, *J* 10 and 1.5), 1.56–2.67 (m, 5 H), 1.16 (d, 3 H, *J* 7); GC–MS: 110, $M^{\bullet +}$; calculated for $C_7H_{10}O$: 110. *2-Methylcyclohex-2-enone*. $\delta_H(CDCl_3)$ 6.01 (br t, 1 H) 1.2–2.6 (m, 9 H); GC–MS: 110, $M^{\bullet +}$; calculated for $C_7H_{10}O$: 110. **2**-*Phenylcyclohex-2-enone*. $\delta_H(CDCl_3)$ 7.30 (br s, 5 H), 6.91 (br t, 1 H), 1.7–2.7 (m, 6 H); GC–MS: 172, $M^{\bullet +}$; calculated for $C_{12}H_{12}O$: 172.

Dichloromethane was purified by repeatedly stirring with a quarter of its volume of concentrated $H_2SO_4$. The acid layer was replaced every 24 h, and the stirring was continued until the lower (acid) layer remained colourless. The upper dichloromethane layer was separated, washed with aqueous 10% sodium hydrogen carbonate, then dried over anhydrous $CaCl_2$. The purified solvent was distilled from calcium hydride under an atmosphere of argon. Acetonitrile was stirred for 24 h with 0.1 wt% $KMnO_4$. The mixture was heated to boiling, cooled and separated from the brown $MnO_2$ residue. The filtered acetonitrile was distilled from $CaH_2$ under an argon atmosphere. The solvents were stored in Schlenk flasks in the dark under an atmosphere of argon.

‡ *J* Values are given in Hz.

**Instrumentation**

The UV–VIS absorption were recorded on a Hewlett-Packard 8450A diode-array spectrometer. The $^1$H NMR spectra were recorded on a JEOL FX 90-Q spectrometer and chemical shifts are reported in ppm units downfield from tetramethylsilane. Gas chromatography was performed on a Hewlett-Packard 5890A series FID gas chromatograph fitted with a model 3392 integrator and a 12.5 m crosslinked dimethylsilicone capillary column. GC–MS analyses were carried out on a Hewlett-Packard 5890 chromatograph interfaced to an HP 5970 mass spectrometer (EI, 70 eV).

The steady-state photolyses were carried out with the focussed beam from a 500 W high-pressure Hg lamp. The beam was passed through a water filter and an appropriate glass cutoff filter (Corning CS series) to remove infrared and ultraviolet light. The sample was contained in a Pyrex Schlenk tube immersed in a water bath at room temperature.

**Charge-transfer excitation of enol silyl ether complexes with chloranil**

In a typical experiment, a solution containing 0.01 M silyl enol ether and 0.01 M chloranil in dichloromethane or acetonitrile (5 ml) was irradiated with the filtered light ($\lambda$ > 500 nm) from a 500 W xenon lamp. After 24 h of continuous photolysis, no colour change was observed. After irradiation, the solvent was stripped *in vacuo*, and the residue was dissolved in $CDCl_3$. An aliquot of 1,2-dichloroethane (10 μl) was added as an internal standard, and the $^1$H NMR spectrum was recorded. The yield of the recovered silyl ether was determined by the integration of its olefinic resonances (at *ca.* 4.9 ppm) against that of the protons of dichloroethane. No new products were detected by $^1$H NMR spectroscopy, and the silyl enol ether was recovered intact in greater than 90% yield. The recovered chloranil was quantitatively determined by GC analysis of the reaction mixture using dodecane as an internal standard, and it was found in at least 95% yield.

**Chloranil-sensitized photooxidation of enol silyl ethers**

Typically, a solution of chloranil and the silyl enol ether (each 0.01 M) in dichloromethane (30 ml) was irradiated with the focussed beam of a 500 W mercury lamp equipped with a 380 nm sharp cutoff filter. As the photolysis proceeded, the solution progressively changed colour from dark orange–yellow to either colourless or pale yellow. After photolysis, the solvent was removed *in vacuo*, and the photolysate was examined by $^1$H NMR and GC–MS. The yields of the enone (**E**) were obtained by GC analysis of the crude photolysate using dodecane as the internal standard. The yields of the adducts (**A**) were obtained by $^1$H NMR integration of the methine protons of the adduct against the resonances of the 1,2-dichloroethane internal standard. The identity of the C–O adducts was verified by their isolation from the crude photolysate as follows. The reaction mixture was repeatedly washed with hexane to remove enone and unreacted silyl enol ether. The solid residue was taken up in dichloromethane and flash chromatographed on a column of silica gel using 95:5 mixture of hexane–ethyl acetate to obtain the adducts. Comparison of the GC–MS of the crude reaction mixture and the isolated adducts showed that desilylation had occurred during chromatographic purification. [O-(2-*Oxocyclohexyl*)]-*tetrachloro*-1,4-*hydroquinone*. $\delta_H(CD_3CN)$ 4.77 (dd, 1 H, *J* 10.6 and 4.6), 1.7–2.5 (m, 8 H); GC–MS: (reaction mixture) 410, 412, 414, 416, $M^{\bullet+}$; calculated for $C_{15}H_{18}Cl_4O_3Si$: 410, 412, 414, 416; (isolated adduct): 338, 340, 342, 344, $M^{\bullet+}$; calculated for $C_{12}H_{10}Cl_4O_3$: 338, 340, 342, 344. O-(2-*Oxocycloheptyl*)*tetrachloro*-1,4-*hydroquinone*. $\delta_H(CD_3CN)$ 4.50 (dd, 1 H, *J* 8.7 and 4.4), 1.65–2.8 (m, 10 H); GC–MS: (reaction mixture) 424, 426, 428, 430, $M^{\bullet+}$; calculated for $C_{16}H_{20}Cl_4O_3Si$: 424, 426, 428, 430; (isolated adduct): 352, 354, 356, 358; calculated for $C_{13}H_{12}Cl_4O_3$: 352, 354, 356, 358. O-[(2-*Oxo*-6-*methylcyclohexyl*)]-*tetrachloro*-1,4-*hydroquinone*. $\delta_H(CD_3CN)$ 4.38 (t, 1 H, *J* 3.7), 0.65–2.5 (m, 10 H); GC–MS: (reaction mixture) 424, 426, 428, 430, $M^{\bullet+}$; calculated for $C_{16}H_{20}Cl_4O_3Si$: 424, 426, 428, 430; (isolated adduct): 352, 354, 356, 358; calculated for $C_{13}H_{12}Cl_4O_3$: 352, 354, 356, 358. O-[(2-*Oxo*-1-*methylcyclohexyl*)]-*tetrachloro*-1,4-*hydroquinone*. $\delta_H(CD_3CN)$ 1.10–2.5 (m, 11 H); GC–MS: (reaction mixture) 424, 426, 428, 430, $M^{\bullet+}$; calculated for $C_{16}H_{20}Cl_4O_3Si$: 424, 426, 428, 430; (isolated adduct): 352, 354, 356, 358; calculated for $C_{13}H_{12}Cl_4O_3$: 352, 354, 356, 358.

**Quantum yields for enol silyl ether loss and α-enone formation**

The photolysis apparatus consisted of a 500 W high pressure xenon lamp (Osram XBO). The focussed output from the lamp was passed through an IR water filter followed by a 360 nm interference filter (10 nm bandpass) used as a monochromator. Calibration of the light flux was carried out using potassium ferrioxalate as the actinometer, according to the method of Hatchard and Parker.[32] The light intensity at 360 nm fell within a range of 5.7–6.1 × $10^{-8}$ Einsteins $min^{-1}$.§ In a typical experiment, a solution of chloranil (0.02 M) and silyl enol ether (0.02 M) was placed in a 1 cm quartz cuvette, which was irradiated for approximately 10 min. The absorbance of the solution at 360 nm was greater than 2.0 throughout the irradiation period. Upon termination of the photolysis, the reaction mixture was quantitatively analysed by gas chromatography, using the internal standard method. The GC response factors for the enone and the silyl ethers were obtained using authentic samples. The quantum yield measurements were repeated three times, and they were found to be reproducible to within 15%.

**Oxidation potentials of enol silyl ethers**

The thermodynamic oxidation potentials ($E^\circ_{ox}$) required for the driving force for electron transfer in Table 5 were estimated from the irreversible (CV) anodic waves of enol silyl ethers **1**–**3**, **7** and **9**[10] by taking cognizance of the facile desilylation[50] of the cation radicals ($ESE^{\bullet+}$) in the following way. The rates of desilylation of enol silyl ether cation radicals $k_{deSi}$ are 5 × $10^3$ times slower in dichloromethane than in acetonitrile.[50] Since $k_{deSi}$ is 2.2 × $10^7$ $s^{-1}$ in acetonitrile,[18] the rate constant in dichloromethane was taken as 4 × $10^3$ $s^{-1}$. The thermodynamic oxidation potential for an EC reaction is given by[51] $E^\circ_{ox} = E_p - 0.78(RT/nF) + (RT/2nF)\ln[(RT/nF)(k/v)]$, where $E_p$ is the (irreversible) cyclic voltammetric peak potential of ESE, $k$ is the rate constant for decomposition of the cation radical and $v$ is the sweep rate in V $s^{-1}$. The anodic peak potentials were recorded previously in dichloromethane at a sweep rate of 0.1 V $s^{-1}$, and are 1.33, 1.41, 1.50 and 1.14 V (*vs.* SCE) for **1**, **2**, **3** and **7**, respectively.[10] The peak potential of **9** was taken to be the same as that of the trimethylsilyl enol ether derived from β-tetralone [3,4-dihydronaphthalen-2(1*H*)-one] (1.10 V). For $k_{deSi} = 4 \times 10^3$ $s^{-1}$ and $v = 0.1$ V $s^{-1}$, the calculation of the oxidation potential, $E^\circ_{ox}$, reduces to ($E_p$ + 0.06 V). The estimated (corrected) values of $E^\circ_{ox}$ are listed in Table 5.

**X-Ray crystallography of adduct 7A from the enol silyl ether of 2-methylcyclohexenone and chloranil**

A clear, colourless prismatic block having approximate dimensions 0.60 × 0.50 × 0.25 mm was mounted in a random orientation on a Nicolet R3m/V automatic diffractometer. The radiation used was Mo-Kα monochromatized by a highly ordered graphite crystal. Final cell constants, as well as other information pertinent to data collection and refinement, are space group: *Pbca* (orthorhombic); cell constants: $a$ = 13.687 (5) Å; $b$ = 11.600 (2) Å, $c$ = 19.140 (4) Å; $V$ = 3093 Å$^3$;

§ 1 Einstein = 1 mol of photons.

molecular formula: $C_{13}H_{12}O_3Cl_4$; formula weight: 358.05; formula units per cell: $Z = 8$; density: $\rho = 1.57$ g cm$^{-3}$; absorption coefficient: $\mu = 7.84$ cm$^{-1}$; radiation (Mo-K$\alpha$): $\lambda = 0.710\,73$ Å; collection range: $4° \leqslant 2\theta \leqslant 50°$; scan width: $\Delta\theta = 1.30 + (K\alpha_2 - K\alpha_1)°$; scan speed range: 1.5–15.0° min$^{-1}$; total data collected: 2601; independent data, $I > 3\sigma(I)$: 2055; total variables: 185; $R = \Sigma||F_o| - |F_c||/\Sigma|F_o|$: 0.035; $R_w = [\Sigma w(|F_o| - |F_c|)^2/\Sigma w|F_o|^2]^{\frac{1}{2}}$: 0.035; weights: $w = \sigma(F)^{-2}$. The Laue symmetry was determined to be *mmm*, and from the systematic absences noted, the space group was shown unambiguously to be *Pbca*. Intensities were measured using the omega scan technique, with the scan rate depending on the count obtained in rapid pre-scans of each reflection. Two standard reflections were monitored after every two hours or every 100 data collected, and these showed no significant change. During the data reduction, Lorentz and polarization corrections were applied. However, no correction for absorption was made due to the small absorption coefficient. The structure was solved by use of the SHELXTL direct methods program, which revealed the positions of all of the non-hydrogen atoms. The usual sequence of isotropic and anistropic refinement was followed, after which all hydrogens were entered in ideal calculated positions and constrained to riding motion, with a single variable isotropic temperature factor for all of them. In the final cycles of least squares the hydroxy hydrogen was allowed to refine freely. After all shift/esd ratios were less than 0.1, convergence was reached at the agreement factors listed above. No unusually high correlations were noted between any of the variables in the last cycle of full-matrix least squares refinement, and the final difference density map showed a maximum peak of about 0.3 e Å$^{-3}$. All calculations were made using Nicolet's SHELXTL PLUS (1987) series of crystallographic programs.¶

¶ Atomic coordinates, thermal parameters and bond lengths and angles have been deposited at the Cambridge Crystallographic Data Centre (CCDC). For details of the deposition scheme, see 'Instructions for Authors', *J. Chem. Soc., Perkin Trans. 2*, 1996, Issue 1. Any request to the CCDC for this material should quote the full literature citation and reference number 188/10.


## Acknowledgements

We thank J. D. Korp for crystallographic assistance, and the National Science Foundation, R. A. Welch Foundation and the Texas Advanced Research Project for financial assistance.


## References


1 P. Brownbridge, *Synthesis*, 1983, 1.
2 M. E. Jung, Y.-G. Pan, M. W. Rathke, D. F. Sullivan and R. P. Woodbury, *J. Org. Chem.*, 1977, **42**, 3961.
3 A. Bhattacharya, L. M. DiMichele, U.-H. Dolling, E. J. J. Grabowski and V. J. Grenda, *J. Org. Chem.*, 1989, **54**, 6118. See also, (*b*) I. Ryu, S. Murai, Y. Hatayama and N. Sonoda, *Tetrahedron Lett.*, 1978, 3455; (*c*) A. Oku, M. Abe and M. Iwamoto, *J. Org. Chem.*, 1994, **59**, 7445.
4 P. A. Evans, J. M. Longmire and D. P. Modi, *Tetrahedron Lett.*, 1995, **36**, 3985.
5 P. Magnus, A. Evans and J. Lacour, *Tetrahedron Lett.*, 1992, **33**, 2933.
6 (*a*) Y. Ito, T. Hirao and T. Saegusa, *J. Org. Chem.*, 1978, **43**, 1011; (*b*) J. Tsuji, I. Minami and I. Shimizu, *Tetrahedron Lett.*, 1983, **24**, 5635.
7 See: T. M. Bockman, S. Perrier and J. K. Kochi, *J. Chem. Soc., Perkin Trans. 2*, 1993, 595 and 1901 for preliminary reports.
8 P. G. Gassman and K. J. Botorff, *J. Org. Chem.*, 1988, **53**, 1097.
9 A. Heidbreder and J. Mattay, *Tetrahedron Lett.*, 1992, **33**, 1973. See also S. Fukuzumi, M. Fujita, J. Otera and Y. Fujita, *J. Am. Chem. Soc.*, 1992, **114**, 10271.
10 Silyl enol ethers have been identified as viable electron donors by a combination of spectral, electrochemical, and photoionization methods. See R. Rathore and J. K. Kochi, *Tetrahedron Lett.*, 1994, **35**, 8577.
11 (*a*) Y. Ito, T. Konoike and T. Saegusa, *J. Am. Chem. Soc.*, 1975, **97**, 649; (*b*) B. B. Snider and T. Kwon, *J. Org. Chem.*, 1992, **57**, 2399; (*c*) E. Baciocchi, A. Casu and R. Ruzzuconi, *Tetrahedron Lett.*, 1989, **30**, 3707.
12 See also (*a*) H. C. Bell, J. T. Pinhey and S. Sternhell, *Aust. J. Chem.*, 1982, **35**, 2237; (*b*) R. M. Moriarty, O. Prakash, M. P. Duncan, R. K. Vaid and H. A. Musallam, *J. Org. Chem.*, 1987, **52**, 150; (*c*) A. N. Kashin, M. L. Tul'chinskii, N. A. Bumagin, I. P. Beletskaya and O. A. Reutov, *J. Org. Chem. USSR (Engl. Transl.)*, 1982, **18**, 1390; (*d*) E. Friederich and W. Lutz, *Chem. Ber.*, **113**, 1245; (*e*) G. A. Olah, L. Ohannesian, M. Arvanaghi and G. K. S. Prakash, *J. Org. Chem.*, 1984, **49**, 2032.
13 (*a*) J. A. Barltrop and B. Hesp, *J. Chem. Soc. C*, 1967, 1625; (*b*) H. P. Trommsdorf and J. Kahane-Paillons, *Spectrochim. Acta, Part A*, 1967, **23**, 1661; (*c*) E. Guerry-Butty, E. Haselbach, C. Pasquier, P. Suppan and D. Phillips, *Helv. Chim. Acta*, 1985, **68**, 912.
14 K. Kawai, Y. Shirota, H. Tsubomura and H. Mikawa, *Bull. Chem. Soc. Jpn.*, 1972, **45**, 77.
15 E. F. Hilinski, S. V. Milton and P. M. Rentzepis, *J. Am. Chem. Soc.*, 1983, **105**, 5193.
16 H. Kobashi, M. Funabashi, T. Kondo, T. Morita, T. Okada and N. Mataga, *Bull. Chem. Soc. Jpn.* 1984, **57**, 3557.
17 (*a*) P. P. Levin, P. F. Pluznikov and V. A. Kuzmin, *Chem. Phys. Lett.*, 1988, **147**, 283; (*b*) E. Baciocchi, T. Del Giacco, F. Elisei and M. Ioele, *J. Org. Chem.*, 1995, **60**, 7974.
18 T. M. Bockman and J. K. Kochi, Part 2, following paper.
19 Compare S. Perrier, S. Sankararaman and J. K. Kochi, *J. Chem. Soc., Perkins Trans. 2*, 1993, 825.
20 H. D. Becker, in *The Chemistry of the Quinonoid Compounds, Part 1*, ed. S. Patai, Wiley, New York, 1974, p. 335.
21 H. D. Becker and A. B. Turner, in *The Chemistry of Quinonoid Compounds*, ed. S. Patai and Z. Rappoport, Wiley, New York, 1988, vol. II, p. 1351.
22 P. P. Fu and R. G. Harvey, *Chem. Rev.*, 1978, **78**, 317.
23 (*a*) M. Bouquet, A. Guy, M. Lemaire and J. P. Guette, *Synth. Commun.*, 1985, **15**, 1153; (*b*) L. Eberson, L. Jönsson and L. G. Wistrand, *Acta Chem. Scand., Ser. B*, 1979, **33**, 413.
24 B. A. McKittrick and B. Ganem, *J. Org. Chem.*, 1985, **50**, 5897.
25 B. Lal, R. M. Gidwani, J. Reden and N. J. deSouza, *Tetrahedron Lett.*, 1984, **25**, 2901.
26 Y. Oikawa, T. Yoshioka and O. Yonemitsu, *Tetrahedron Lett.*, 1982, 889.
27 E. Gebert, A. H. Reis Jr., J. S. Miller, H. Rommelmann and A. J. Epstein, *J. Am. Chem. Soc.*, 1982, **104**, 4403.
28 K. Maruyama and A. Osuka, in Ref. 21, p. 759. See also Barltrop *et al.* in Ref. 13.
29 C. S. Sharma, S. C. Sethi and S. Dev, *Synthesis*, 1974, 45.
30 D. Knausz, A. Meszticzky, L. Szakacs, B. Csakvari and K. Ujszaszy, *J. Organometal. Chem.*, 1983, **256**, 11.
31 C. Reichardt, *Solvents and Solvent Effects in Organic Chemistry*, VCH, New York, 2nd edn., 1988.
32 C. G. Hatchard and C. A. Parker, *Proc. Royal Soc. London Ser. A*, 1956, 518.
33 See: S. Perrier *et al.* in Ref. 19.
34 Note that the absorption spectra in Fig. 1 show that the CT absorbance is negligible compared to the local excitation of chloranil, especially under the conditions of the preparative photoreactions in Tables 1 and 2.
35 T. Clark, *J. Am. Chem. Soc.*, 1987, **109**, 6838.
36 See also H. D. Roth, *Top. Curr. Chem.*, 1992, **163**, 160.
37 D. Rehm and A. Weller, *Ber. Bunsenges. Phys. Chem.*, 1969, **73**, 834.
38 For the (estimated) value of $E°_{ox}$ from the anodic CV peak potential (Rathore *et al.* in Ref. 10), see Experimental section.
39 (*a*) C. K. Mann and K. K. Barnes, *Electrochemical Reactions in Nonaqueous Systems*, Dekker, New York, 1970; (*b*) S. L. Murov, I. Carmichael and G. L. Hug, *Handbook of Photochemistry*, Dekker, New York, 2nd edn., 1993, p. 19.
40 R. Gschwind and E. Haselbach, *Helv. Chim. Acta*, 1979, **62**, 941; see also Refs. 14–17.
41 (*a*) Y. Hirata, Y. Kanda and N. Mataga, *J. Phys. Chem.*, 1983, **87**, 1659; (*b*) T. Asahi and N. Mataga, *J. Phys. Chem.*, 1989, **93**, 6575; (*c*) T. Asahi, N. Mataga, Y. Takahashi and T. Miyashi, *Chem. Phys. Lett.*, 1990, **171**, 309; (*d*) H. Miyasaka, K. Morita, K. Kamada and N. Mataga, *Bull. Chem. Soc. Jpn.*, 1990, **63**, 3385; (*e*) T. Asahi and N. Mataga, *J. Phys. Chem.*, 1991, **95**, 1956.
42 P. R. Rich and D. S. Bendall, *Biochim. Biophys. Acta*, 1980, **592**, 506.
43 (*a*) H. Segawa, C. Takehara, K. Honda, T. Shimidzu, T. Asahi and

N. Mataga, *J. Phys. Chem.*, 1992, **96**, 503; (*b*) T. Asahi, M. Ohkohchi and N. Mataga, *J. Phys. Chem.*, 1993, **97**, 13132.
44 (*a*) I. R. Gould, L. J. Mueller and S. Farid, *Z. Phys. Chem.*, 1991, **170**, 143; (*b*) I. R. Gould, R. W. Young, L. J. Mueller and S. Farid, *J. Am. Chem. Soc.*, 1994, **116**, 8176; (*c*) I. R. Gould, R. H. Young, L. J. Mueller, A. C. Albrecht, S. Farid, *J. Am. Chem. Soc.*, 1994, **116**, 8188; (*d*) A. B. Myers, *Chem. Phys.*, 1994, **180**, 215.
45 This trend ('inverted' as opposed to the 'normal' increase in rate with increasing driving force) is predicted by the Marcus theory of electron transfer. See (*a*) R. A. Marcus, *J. Chem. Phys.*, 1965, **43**, 679; (*b*) P. Suppan, *Top. Curr. Chem.*, 1992, **163**, 95.
46 See H. D. Roth, *Acc. Chem. Res.*, 1987, **20**, 343.
47 Intersystem crossing in radical pairs [occurring on a timescale of nanoseconds and modulated by external or internal (nuclear) magnetic fields] plays a central role in the development of CIDNP and CIDEP. See (*a*) R. Kaptein, *Adv. Free-Radical Chem.*, 1975, **5**, 381; (*b*) R. G. Lawler, *Acc. Chem. Res.*, 1972, **5**, 25; (*c*) A. L. Buchachenko, *Russ. Chem. Rev.*, 1976, **45**, 375.
48 P. Cazeau, F. Duboudin, F. Moulines, O. Babot and J. Dunogues, *Tetrahedron*, 1987, **43**, 2075.
49 I. Fleming and I. Paterson, *Synthesis*, 1979, 736.
50 M. Schmittel, M. Keller and A. Burghart, *J. Chem. Soc. Perkin Trans. 2*, **1995**, 2327.
51 A. J. Bard and L. R. Faulkner, *Electrochemical Methods*, Wiley, New York, 1980, p. 453.

*Paper* 6/00833J
*Received* 5*th February* 1996
*Accepted* 29*th March* 1996